Effective and magnetic interactions in the $3d^N$ configurations of the fifth spectra of the iron group

Z. B. Goldschmidt and Z. Vardi
Racah Institute of Physics, The Hebrew University of Jerusalem, Jerusalem 91904, Israel
(Received 4 September 1984)

A systematic investigation was conducted on the effects of the effective and magnetic interactions on the energy-level schemes of the $3d^N$ configurations ($N=2,3,\ldots,8$) in the fifth spectra of the iron group. The interactions considered were the effective electrostatic interaction described by α, β, T, and T_x, the mutual magnetic spin-other-orbit and spin-spin interactions parametrized by M^0 and M^2, and the effective electrostatic—spin-orbit (effective EL-SO) interaction represented by Q^2 and Q^4. The values of the various radial integrals were determined by using both *ab initio* and semiempirical methods. The introduction of all above-mentioned "weak" interactions greatly improved the fit between theory and experiment, concerning both the term values and the multiplet splittings. Close agreement prevails between corresponding parameter values obtained in the semiempirical and in the *ab initio* methods. All parameters vary with N (along the row) in a smooth and regular manner; in particular, the variations of the spin-dependent parameters agree with their theoretical dependence on the effective nuclear charge. All the above results crucially depend on the simultaneous introduction of all parameters representing perturbations of the same type and order, that is, all effective electrostatic parameters should simultaneously be introduced in one stage and all the spin-dependent weak interactions should simultaneously be introduced in a subsequent stage.

I. INTRODUCTION

In the years 1968—1974, systematic investigations were conducted on the effects of the effective and mutual magnetic interactions on the energy-level structure of the $3d^N$ configurations ($N=2,3,\ldots,8$) in the third and fourth spectra of the iron group.[1—4] The interactions considered (in addition to the conventional electrostatic and spin-orbit interactions) were the following.

(1) The two- and three-electron effective electrostatic interaction described, respectively, by $\alpha L(L+1)+\beta Q$ (Refs. 5—13) and $tT+t_xT_x$ (Refs. 12—19). This interaction represents, to second-order perturbation theory, electrostatic interaction with distant configurations.

(2) The spin-spin (ss) and the spin-other-orbit (soo) interactions, described by the parameters M^0 and M^2. These belong to the category of the mutual magnetic interactions;[20—26] they, respectively, represent the mutual interaction between the magnetic dipole moments of the electrons, and between the dipole moment of one electron and the orbital motion of the other.

(3) The effective electrostatic—spin-orbit (effective EL-SO) interaction, described by Q^2 and Q^4; it represents, to second-order perturbation theory, the mixed electrostatic—spin-orbit interaction with distant configurations.

The effective electrostatic interaction is spin-independent, and affects the term structure of an LS-coupled configuration. On the other hand, the mutual magnetic and effective EL-SO interactions are spin-dependent, thus affecting the multiplet splittings; in the present paper, these interactions will be referred to as "additional spin-dependent interactions" (additional SDI). Generally, the effective electrostatic interaction is stronger than the additional SDI; this relation is to be expected on considering the origin of these two groups of interactions. The effective electrostatic and the additional SDI will from now on be grouped together under the title "weak interactions."

In the above-mentioned investigations it was shown that the inclusion of the "weak" interactions in the energy-level calculations greatly improves the fit between theory and experiment, concerning both the term structure and the multiplet splittings. Furthermore, consistent and reliable values were obtained for the various radial integrals (parameters); these values exhibit a regular and smooth variation with the number N of the d electrons.

Investigations on the effects of the weak interactions on the following nf^N configurations in lanthanide and actinide ions were also carried out: the $4f^2$ configuration in Pr IV (Refs. 1, 4, 27, and 28) and Ce III,[27,28] the $4f^3$ configuration in Pr III,[1,4,28,29] and the $5f^2$ configuration in U V.[30,31] A survey of the studies in the field of the additional SDI in heavy atoms, up to the beginning of 1970, was published by Judd.[32] A detailed discussion of the effects of the weak interactions on various lanthanide spectra is included in Ref. 28. However, because of the lack of experimental data in the lanthanide and actinide ions, none of these investigations was comprehensive so as to include a complete group of configurations, as compared to the above-mentioned investigations on the $3d^N$ configurations of the third and fourth spectra of the iron group.

Recently, the experimental analyses of the fourth to sixth spectra of the iron group have been greatly extended by measuring spectral transitions in the vuv region. Thus, the energy level lists of the ground $3d^N$ configurations of

these spectra have become almost complete. It is, therefore, possible to extend the theoretical investigation of the weak interactions to these newly measured spectra.

In the present work, the configurations chosen for this investigation are the $3d^N$ configurations of the fifth spectra of the iron group. These are Cr V $3d^2$,[33] Mn V $3d^3$,[34] Fe V $3d^4$,[35] Co V $3d^5$,[36] Ni V $3d^6$,[37] Cu V $3d^7$,[38] and Zn V $3d^8$.[39] 160 out of 161 levels belonging to these configurations were experimentally located (see Refs. 33—39). The only missing level is Ni V $3d^6\,{}^1_0S_0$.

Since, as mentioned above, the effective electrostatic interaction is stronger than the additional SDI, the study of the effects of the weak interactions on the energy-level structure of these configurations was carried out in two stages: in the first stage only the effective electrostatic interaction represented by $\alpha L(L+1)+\beta Q+tT+t_xT_x$ was included, in addition to the traditional "real" electrostatic and spin-orbit interactions. The additional SDI, described by the M^k and Q^k, were introduced in the second stage.

Energy-level calculations of these configurations were carried out by several authors: Cr V $3d^2$,[40] Mn V $3d^3$,[40] Fe V $3d^4$,[35,40] Co V $3d^5$,[36] Ni V $3d^6$,[37] Cu V $3d^7$,[38,40] Zn V $3d^8$.[39] The results of these calculations, with the exception of Zn V $3d^8$, are summarized and discussed in a recent paper by Hansen and Raassen.[40] In all these calculations, only α, β, and T were included, whereas T_x and the additional SDI were neglected. Since α, β, T, and T_x are neither orthogonal to each other nor to the real electrostatic parameters,[41] the omission of T_x was reflected in the calculated values of all real and other effective electrostatic parameters. In particular, it resulted in an irregular behavior of the values obtained for β, along the group, and also obscured the mode of change of T, as specified below.

In the first stage of the present work, it is shown that the introduction of T_x is important from two points of view: (1) it results in values for all electrostatic parameters which vary regularly and smoothly with N; (2) in all configurations where T_x is meaningful (that is, in d^3, d^4, d^6, and d^7), it significantly improves the fit between observed and calculated levels. Thus, in order to obtain meaningful results, all effective electrostatic parameters should be introduced simultaneously.

In the second stage of the present work, the subsequent inclusion of the additional SDI greatly improved the fit between observed and calculated multiplet splittings. Reliable and consistent values of the appropriate parameters were determined, which agree remarkably well with theoretical predictions.

II. OPERATORS AND RADIAL INTEGRALS (PARAMETERS) FOR $(nl)^N$ CONFIGURATIONS

A. Effective electrostatic interaction

The properties of this interaction, from a theoretical point of view, were extensively studied by Rajnak and Wybourne,[12] by Racah and Stein,[13] and by Judd.[42] Five types of perturbing configurations contribute to the effective electrostatic operator of a perturbed configuration $(nl)^N$. These are as follows:

1(a), $(nl)^{N-2}(n'l')^2$; 1(b), $(nl)^{N-2}n'l'n''l''$;

2(a), $(n'l')^{4l'}(nl)^{N+2}$;

2(b), $(n'l')^{4l'+1}(n''l'')^{4l''+1}(nl)^{N+2}$;

3, $(n'l')^{4l'+1}(nl)^Nn''l''$;

4, $(nl)^{N-1}n'l'$;

5, $(n'l')^{4l'+1}(nl)^{N+1}$.

Each perturbing configuration belonging to types 1—3 has two "new" electrons (holes) compared with $(nl)^N$ (a new hole plays the same role as a new electron). Consequently, its contribution to the effective electrostatic interaction is described by a two-electron operator. For instance, for a perturbing configuration of the type 1(a) this operator is given by

$$H^{(2)}_{\text{eff}}=-\sum_t(2t+1)M(t;ll,l'l')\sum_{i<j}(\underline{u}^{(t)}_i\cdot\underline{u}^{(t)}_j)\,, \tag{1}$$

where $\underline{u}^{(t)}$ is the unit tensor operator defined by Racah,[43]

$$(nl||\underline{u}^{(t)}||nl)=1\,, \tag{2}$$

and $M(t;ll,l'l')$ is defined by the following formula:[12]

$$M(t;l_al_b,l_cl_d)=\sum_{k,k'}\begin{Bmatrix}k & k' & t\\ l_a & l_b & l_c\end{Bmatrix}\begin{Bmatrix}k & k' & t\\ l_a & l_b & l_d\end{Bmatrix}\times P(kk';l_al_b,l_cl_d)\,, \tag{3}$$

where

$$P(kk';l_al_b,l_cl_d)=R^k(l_al_b,l_cl_d)R^{k'}(l_al_b,l_cl_d)\times(l_a||\underline{C}^{(k)}||l_c)(l_b||\underline{C}^{(k)}||l_d)\times(l_a||\underline{C}^{(k')}||l_c)(l_b||\underline{C}^{(k')}||l_d)/\Delta E\,, \tag{4}$$

$R^k(l_al_b,l_cl_d)$ and $R^{k'}(l_al_b,l_cl_d)$ being Slater integrals, and ΔE is the (positive) energy separation between the perturbing and the perturbed configurations. In formula (1), t may take the values $0<t\leq 2l$. However, for even values of t, the coefficients of $M(t;ll,l'l')$ have the same angular dependence as the coefficients of the Slater integrals describing the real electrostatic interaction within the l^N configuration. Therefore, only $M(t;ll,l'l')$ with odd values of t constitute independent parameters. The number of these parameters is l, compared with $l+1$, the number of real Slater parameters. For d^N configurations, t may take the values 1 and 3. Following Trees[5] and Racah,[6] the two-electron effective electrostatic operator is written in the form

$$\alpha L(L+1)+\beta Q\,,$$

where Q stands for the eigenvalues of the seniority operator.[44] α and β are given by the following expressions:[12,40]

$$\alpha=[M(1;ll,l'l')-M(3;ll,l'l')]/20\ ,$$
$$\beta=-M(3;ll,l'l')\ . \tag{5}$$

(the expression given in Ref. 12 should be divided by a factor of 2). In semiempirical (SI) calculations, α and β are treated as adjustable parameters.

Each perturbing configuration of type 4 or 5 has only one new electron (hole), compared with $(nl)^N$. Consequently, its contribution is described by a sum of three-, two-, and one-electron terms:

$$H^3_{\rm eff}(l^{N-1}l')=-\sum_{k,k',k''}P(kk';ll,ll')\left[(2k''+1)\begin{Bmatrix}k & k' & k''\\ l & l & l'\end{Bmatrix}[\underline{U}^{(k)}\times\underline{U}^{(k'')}\times\underline{U}^{(k')}]^{(0)}\right.$$
$$\left.+[\delta_{ll'}/(2l+1)][(\underline{U}^{(k)}\cdot\underline{U}^{(k)})+(\underline{U}^{(k')}\cdot\underline{U}^{(k')})-N/(2l+1)]\right]$$
$$=\sum_{k,k'}P(kk';ll,ll')\phi_e(kk';ll,ll')\ , \tag{6}$$

$$H^3_{\rm eff}[(l')^{4l'+1}l^{N+1}]=-\sum_{k,k',k''}P(kk';ll,ll')$$
$$\times\left[(-1)^{k''+1}(2k''+1)\begin{Bmatrix}k & k' & k''\\ l & l & l'\end{Bmatrix}[\underline{U}^{(k)}\times\underline{U}^{(k'')}\times\underline{U}^{(k')}]^{(0)}-[2\delta_{kk'}/(2k+1)](\underline{U}^{(k)}\cdot\underline{U}^{(k)})\right]$$
$$=\sum_{k,k'}P(kk';ll,ll')\phi_h(kk';ll,ll')\ . \tag{7}$$

In these formulas

$$\underline{U}^{(k)}=\sum_i \underline{u}_i^{(k)}\ ;$$

k and k' may take all even nonzero integer values that obey the triangular conditions required by the $6j$ symbol. k'' may assume all nonzero integer values consistent with the same triangular conditions.

Judd[16] and Feneuille[17] have shown, that for d^N configurations, only two of the $P(kk';ll,ll')$ appearing in (6) and (7) constitute independent parameters. Following Trees[14] and Shadmi *et al.*,[18] $H^3_{\rm eff}$ is given as $tT+t_xT_x$; these two terms were chosen for $3d^N$, so as to represent interactions with the special perturbing configurations $3s\,3p^6 3d^{N+1}$ and $3d^{N-1}n'd$, respectively. Thus, the expression for tT is obtained from formula (7) by the substitutions $k=k'=2$, $l=2$, $l'=0$; more specifically, T is defined as

$$T=-P(22;22,20)/1750\ , \tag{8}$$

which gives

$$t=-1750\phi_h(22;22,20)\ . \tag{9}$$

In the same manner the expression for t_xT_x is obtained by substituting in formula (6) $k=k'=2$, $l=l'=2$; T_x and t_x are then defined as

$$T_x=-P(22;22,22)/1750\ , \tag{10}$$
$$t_x=-1750\phi_e(22;22,22)\ . \tag{11}$$

In SI calculations, T and T_x are treated as adjustable parameters.

B. Mutual magnetic interactions

The operators representing the ss and the soo interactions for $(nl)^N$ configurations are given, in tensor-operator form, by the following formulas:[45,3,4,28,30]

$$H_{\rm ss}=-\beta^2(5)^{-1/2}\sum_k(-1)^k\left[\frac{(2k+5)!}{(2k)!}\right]^{1/2}\sum_{i\neq j}\left[\frac{r_j^k}{r_i^{k+3}}([\underline{C}_i^{(k+2)}\times\underline{C}_j^{(k)}]^{(2)}\cdot[\underline{s}_i\times\underline{s}_j]^{(2)})\right.$$
$$\left.+\frac{r_i^k}{r_j^{k+3}}([\underline{C}_i^{(k)}\times\underline{C}_j^{(k+2)}]^{(2)}\cdot[\underline{s}_i\times\underline{s}_j]^{(2)})\right]\ , \tag{12}$$

$$H_{\rm soo}=\beta^2 2(3)^{-1/2}\sum_k(-1)^k\sum_{i\neq j}\left[\frac{r_i^{k-2}}{r_j^{k+1}}(2k+1)(2k-1)^{1/2}[\underline{C}_j^{(k)}\times[\underline{C}^{(k)}\times\underline{l}]_i^{(k-1)}]^{(1)}\right.$$
$$\left.-\frac{r_j^k}{r_i^{k+3}}(2k+1)(2k+3)^{1/2}[\underline{C}_j^{(k)}\times[\underline{C}^{(k)}\times\underline{l}]_i^{(k+1)}]^{(1)}\right]\cdot(\underline{s}_i+2\underline{s}_j) \tag{13}$$

TABLE I. Electrostatic parameters, "real" and effective, in cm^{-1} (*ab initio*, LS2, and GLS2).

Parameter	Cr V $3d^2$	$\frac{P_{GLS}}{P_{HF}}$	Mn V $3d^3$	$\frac{P_{GLS}}{P_{HF}}$	Fe V $3d^4$	$\frac{P_{GLS}}{P_{HF}}$
A_{LS}	8754±0		17384±1		25714±21	
A_{GLS}	8762±21		17385±20		25736±17	
B_{LS}	1108±0		1161±0		1212±1	
B_{GLS}	1109	(0.876)	1161	(0.871)	1213	(0.866)
B_{HF}	1266		1333		1400	
C_{LS}	4039±0		4293±1		4559±6	
C_{GLS}	4033	(0.844)	4296	(0.855)	4559	(0.865)
C_{HF}	4779		5024		5268	
α_{LS}	33.9±0.0		37.6±0.1		40.8±1.0	
α_{GLS}	33.6		37.1		40.6	
β_{LS}	−444±0		−419±2		−396±15	
β_{GLS}	−443.0		−426.5		−410.0	
T_{LS}	[−7.57]		−7.33±0.01		−7.14±0.09	
T_{GLS}	−7.57		−7.37		−7.17	
$(T_x)_{LS}$	[−0.15]		−0.81±0.02		−0.82±0.13	
$(T_x)_{GLS}$	−0.15		−0.52		−0.89	
F^2_{LS}	82565		86940		91301	
F^2_{GLS}	82572	(0.865)	86961	(0.865)	91350	(0.866)
F^2_{HF}	95466		100500		105482	
F^4_{LS}	50891		54092		57443	
F^4_{GLS}	50816	(0.844)	54130	(0.855)	57443	(0.865)
F^4_{HF}	60210		63307		66373	
$(F^2/F^4)_{LS}$	1.62		1.61		1.59	
$(F^2/F^4)_{GLS}$	1.62		1.61		1.59	
$(F^2/F^4)_{HF}$	1.59		1.59		1.59	

with $\beta=e\hbar/2mc$.

The appropriate radial integrals (parameters) describing these interactions are those defined by Marvin:[22]

$$M^k=\frac{\beta^2}{2}\int_0^\infty\int_0^\infty \frac{r_<^k}{r_>^{k+3}}R^2_{nl}(r_1)R^2_{nl}(r_2)dr_1dr_2\ , \quad (14)$$

where $r_<=\min(r_1,r_2)$ and $r_>=\max(r_1,r_2)$. For d electrons k may take the values 0,2.

C. Effective EL-SO interaction

At the outset, three types of perturbing configurations may contribute to the effective EL-SO operator, each of them differing from $(nl)^N$ by the principal quantum number n of one electron only. These are

(i) $(nl)^{N-1}n'l$,

(ii) $(n'l)^{4l+1}(nl)^{N+1}$,

(iii) $(n'l')^{4l'+1}(nl)^N n''l'$.

After omitting terms proportional to the spin-orbit interaction, it is found that only the contributions of (i) and (ii) remain, whereas that of (iii) vanishes. In the present work, with investigated configurations of the type $3d^N$, configurations of type (ii) do not exist; thus, only the contribution of (i) should be taken into account. In this case, $H_{\text{EL-SO}}$ is given by the following expression:[3,28]

$$H_{\text{EL-SO}}=-2\sum_{k\ \text{even}>0} Q^k[l(l+1)(2l+1)]^{1/2}(2k+1)^{-1/2} \times\sum_{t\ \text{odd}}(2t+1)\begin{Bmatrix}1 & k & t\\ l & l & l\end{Bmatrix} \times(\underline{U}^{(k)}\cdot\underline{T}^{(1t)k})\ , \quad (15)$$

where $T^{(1t)k}=\sum_i t_i^{(1t)k}=\sum_i[\underline{s}_i\times\underline{u}_i^{(t)}]^{(k)}$. The parameters Q^k are defined as follows:

$$Q^k=(l||\underline{C}^{(k)}||l)^2\sum_{n'}\frac{R^k(nlnl,nln'l)\zeta_{nl,n'l}}{\Delta E_{n,n'}} \quad (16)$$

with $R^k(nlnl,nln'l)$ and $\zeta_{nl,n'l}$ being, respectively, Slater and spin-orbit parameters, and $\Delta E_{n,n'}$ is the (positive) energy separation between the perturbing and the perturbed configurations. For d electrons, k may take the values 2,4. Formulas for the matrix elements of the additional SDI for $(nl)^N$ configurations are given in Refs. 3 and 28.

Co V $3d^5$	$\frac{P_{GLS}}{P_{HF}}$	Ni V $3d^6$	$\frac{P_{GLS}}{P_{HF}}$	Cu V $3d^7$	$\frac{P_{GLS}}{P_{HF}}$	Zn V $3d^8$	$\frac{P_{GLS}}{P_{HF}}$
43 644±35		27 860±17		21 204±7		12 420±0	
43 597±11		27 861±16		21 251±11		12 433±18	
1265±1		1316±1		1365±0		1419±0	
1264	(0.862)	1318	(0.860)	1368	(0.856)	1420	(0.854)
1467		1532		1598		1663	
4817±5		5086±5		5359±3		5620±0	
4822	(0.875)	5085	(0.885)	5348	(0.893)	5611	(0.902)
5509		5749		5987		6223	
44.6±0.7		47.1±0.6		51.8±0.4		54.9±0.0	
44.1		47.6		51.1		54.6	
−396±8		−379±12		−367±4		−351±0	
−393.5		−377.0		−360.5		−344.0	
[−6.97]		−6.83±0.06		−6.51±0.04		[−6.37]	
−6.97		−6.77		−6.57		−6.37	
[−1.26]		−1.73±0.10		−1.53±0.06		[−2.37]	
−1.26		−1.63		−2.00		−2.37	
95 704		100 086		104 398		108 871	
95 690	(0.867)	100 177	(0.869)	104 468	(0.869)	108 857	(0.870)
110 423		115 328		120 203		125 053	
60 694		64 084		67 523		70 812	
60 757	(0.875)	64 071	(0.885)	67 385	(0.893)	70 699	(0.902)
69 413		72 432		75 432		78 416	
1.58		1.56		1.55		1.54	
1.58		1.56		1.55		1.54	
1.59		1.59		1.59		1.59	

III. ENERGY-LEVEL CALCULATIONS

A. *Ab initio* evaluation of the various interaction parameters

In order to obtain a preliminary and independent information on the values of the various interaction parameters, Hartree-Fock[46] (HF) and parametric potential[47] (PP) calculations were performed for all $3d^N$ configurations of the fifth spectra of the iron group. These calculations resulted in numerical values for ζ_{3d}, M^0, M^2, and also for the Slater parameters $F^k(3d,3d)$ $(k=2,4)$, from which the parameters B and C, defined by Racah,[43] could be evaluated. Since the use of both methods resulted in very close values for all corresponding parameters, only those obtained by the HF method are listed in Tables I and II.

For estimating the orders of magnitude of the effective EL-SO parameters Q^2 and Q^4 for each investigated configuration $3d^N$ $(N=2-8)$, the contributions of the perturbing configurations $3d^{N-1}nd$ $(n=4-9)$ were evaluated, through a further use of the PP program: numerical values were obtained for the parameters $R^k(3d\,3d,3dnd)$, $\zeta_{3d,nd}$, and for the energy difference $\Delta E_{3d,nd}$ $(k=2,4;$ $n=4-9)$; these were then used to evaluate $Q^k(3d,nd)$ $(k=2,4;$ $n=4-9)$ according to the definition given in formula (16) above. All these values are listed in Tables XVI–XXII at the end of this paper. Each of these tables also includes, in its lower row, the sum of all contributions to the Q^k's, to the right of the heading "Q^k total." Since the individual Q^k values strongly decrease with n, it is assumed that the Q^k-total values reasonably approximate the orders of magnitude of the respective Q^k's. These values are also listed in Table II.

No attempt was made here to evaluate the effective electrostatic parameters through the use of the HF and the PP methods. Detailed discussion of this subject can be found in Ref. 40.

B. Semiempirical calculations

The energy levels and the parameter values of the investigated configurations were then calculated, in the SI method, by using the diagonalization–least-squares procedure. As mentioned in the Introduction, these calculations were performed in two stages: in the first stage, only the effective electrostatic interaction was introduced, in addition to the traditional interactions; the additional SDI were added in the second stage, when the effects of the effective electrostatic interaction on the energy-level structure of these configurations were completely understood.

TABLE II. SDI parameters, in cm^{-1} (*ab initio*, LS2, and GLS2).

Parameter	Cr V $3d^2$	$\frac{P_{GLS}}{P_{ab\ initio}}$	Mn V $3d^3$	$\frac{P_{GLS}}{P_{ab\ initio}}$	Fe V $3d^4$	$\frac{P_{GLS}}{P_{ab\ initio}}$
ζ_{LS}	335±0		427±1		540±9	
ζ_{GLS}	336	(1.009)	425	(0.998)	534	(0.994)
ζ_{HF}	333		426		537	
M^0_{LS}	2.003±0.000		2.118±0.069		2.701±1.007	
M^0_{GLS}	1.564	(0.946)	1.943	(0.990)	2.332	(1.012)
M^0_{HF}	1.653		1.962		2.305	
M^2_{LS}	1.012±0.000		0.987±0.054		1.864±1.099	
M^2_{GLS}	0.714	(0.779)	0.917	(0.844)	1.120	(0.878)
M^2_{HF}	0.916		1.086		1.275	
Q^2_{LS}	8.8±0.0		34.1±2.3		45.2±31.8	
Q^2_{GLS}	19.4	(0.83)	29.2	(1.03)	39.0	(1.14)
Q^2_{PP}	23.4		28.4		34.3	
Q^4_{LS}	[6.0]		[23.2]		[30.7]	
Q^4_{GLS}	[13.2]		[19.1]		[26.5]	
Q^4_{PP}	16.0		19.4		23.4	
$(M^0/M^2)_{LS}$	1.98		2.15		1.45	
$(M^0/M^2)_{GLS}$	2.19		2.12		2.07	
$(M^0/M^2)_{HF}$	1.80		1.81		1.81	
$(Q^4/Q^2)_{PP}$	0.68		0.68		0.68	
Δ_{LS2}	0.00		2		33	
Δ_{GLS2}						
Δ_{LS1}	14		21		39	
Δ_{GLS1}						

In each of these stages, the calculations were conducted in two steps. In the first step, each configuration was treated separately. Such calculations will from now on be referred to as LS calculations. In these calculations, in either stage, it was found that the parameters representing the various interactions vary regularly from one spectrum to the other along the row. This conclusion was also confirmed on inspecting the *ab initio* values obtained for the various parameters. Thus it was possible in the next step to perform a general least-squares (GLS) calculation, treating all the $3d^N$ configurations as a single problem, the radial parameters being restricted to change from one spectrum to another according to a simple interpolation formula. For any interaction parameter P, the interpolation formula was of the form

$$P = P_0 + P_1 x + P_2 y$$

in which $x = N - 5$ and $y = x^2 - 4$. The coefficients P_0, P_1, and P_2 of the interpolation formulas now served as free parameters. In most cases a linear change was sufficient ($P_2 = 0$). From now on, the results relating to the first and second stages will be referred to as LS1 and GLS1, and LS2 and GLS2, respectively.

In the separate LS1 and LS2 calculations of d^2, d^5, and d^8, T and T_x had to be fixed, because in the two-electron (hole) configurations and, to a good approximation, also in half-filled-shell configurations, these parameters are linear combinations of other electrostatic parameters. In all second-stage calculations the following restrictions were imposed on the additional SDI parameters:

(i) $M^k_{ss} = M^k_{soo}$,

(ii) $Q^4/Q^2 = 0.68$.

The first restriction follows directly from the definition of the M^ks; the second restriction is suggested by the constancy of the ratio $(Q^4/Q^2)_{PP}$ obtained in the PP calculations for the various d^N configurations [see row entitled $(Q^4/Q^2)_{PP}$ in Table II], and from a set of LS and GLS calculations performed with free Q^k's.

In both GLS1 and GLS2 calculations all the parameters except ζ_{3d} were constrained to change linearly with N; for ζ_{3d} a quadratic correction term was also included.

The parameter values obtained in GLS1 and GLS2 are given in Table III, together with their appropriate mean errors Δ. Inspection of this table shows that the electrostatic parameters both real and effective, and the spin-orbit parameters, have not changed significantly on the introduction of the additional SDI.

The electrostatic and spin-dependent parameter values obtained in LS2 and GLS2 for the individual configuration are listed in Tables I and II respectively, in consecutive rows with the corresponding *ab initio* values. For each of the real electrostatic and spin-dependent parameters, the ratio $P_{GLS}/P_{ab\ initio}$ is also shown (in parentheses). Table I also includes the ratios F^2/F^4; Table II includes the ratios M^0/M^2 and Q^4/Q^2 and the

TABLE II. (*Continued*).

Co V $3d^5$	$P_{GLS}/P_{ab\ initio}$	Ni V $3d^6$	$P_{GLS}/P_{ab\ initio}$	Cu V $3d^7$	$P_{GLS}/P_{ab\ initio}$	Zn V $3d^8$	$P_{GLS}/P_{ab\ initio}$
654±11		810±6		978±2		1166±0	
664	(0.994)	813	(0.991)	982	(0.986)	1171	(0.977)
668		820		996		1198	
2.288±0.792		3.297±0.642		3.785±0.241		4.457±0.000	
2.701	(1.006)	3.080	(0.994)	3.459	(0.973)	3.838	(0.948)
2.684		3.100		3.554		4.049	
1.374±1.023		1.847±0.754		1.619±0.164		2.196±0.000	
1.323	(0.892)	1.526	(0.891)	1.729	(0.881)	1.932	(0.865)
1.483		1.712		1.962		2.234	
32.5±30.0		63.2±21.4		72.0±6.4		131.8±0.0	
48.8	(1.20)	58.6	(1.27)	68.4	(1.28)	78.2	(1.28)
40.5		46.1		53.2		61.2	
[22.1]		[43.0]		[49.0]		[89.6]	
[33.2]		[39.8]		[46.5]		[53.2]	
27.5		31.4		36.1		41.2	
1.67		1.79		2.34		2.03	
2.04		2.02		2.00		1.99	
1.81		1.81		1.81		1.81	
0.68		0.68		0.68		0.67	
37		22		5		0	
27							
44		34		33		47	
35							

mean errors Δ_{LS2} and Δ_{GLS2}; Δ_{LS1} and Δ_{GLS1} are also given, for comparison.

The calculated values of the energy levels as obtained in GLS2 are given in Tables IV–X, together with the observed levels, the deviations $O_i - C_i$ between observed and calculated levels, and the composition percentages of the eigenstates. The last column of each of these tables comprises the $O_i - C_i$ values as obtained in GLS1, for comparison.

IV. RESULTS AND CONCLUSIONS

A. Stage 1: The need for a complete set of effective electrostatic parameters

1. Improvement of the fit between observed and calculated levels

In stage 1, the GLS1 calculations were carried out with 160 levels against 22 parameters (see the second column of Table III). The good agreement obtained between theory and experiment is reflected in the small mean error, being 35 cm^{-1}.

Table XI includes both the mean errors Δ_{LS1}, obtained in the individual LS1 calculations, and the mean errors $\Delta_{\alpha\beta T}$, obtained on neglecting T_x.[35–40] On comparing the corresponding values of Δ_{LS1} and $\Delta_{\alpha\beta T}$, the importance of T_x can immediately be deduced: in all configurations where the introduction of this parameter is meaningful, that is in d^3, d^4, d^6, and d^7, the mean errors significantly reduced, as shown below.

For d^3,

$$27\ cm^{-1} \rightarrow 21\ cm^{-1} = 78\% \text{ of its former value},$$

for d^4,

$$58\ cm^{-1} \rightarrow 39\ cm^{-1} = 67\% \text{ of its former value},$$

for d^6,

$$78\ cm^{-1} \rightarrow 34\ cm^{-1} = 44\% \text{ of its former value},$$

and for d^7,

$$\left\{\begin{matrix}57\\55\end{matrix}\right\}\ cm^{-1} \rightarrow 33\ cm^{-1} = \left\{\begin{matrix}58\%\\60\%\end{matrix}\right\} \text{ of its former value}.$$

In the present work, no attempt was made to perform LS or GLS calculations in pure intermediate coupling, that is, on completely neglecting the effective electrostatic parameters α, β, T, and T_x. A performance of such calculations would bring us back to the 1950s, when Trees[5] [before introducing his $\alpha L(L+1)$ correction] obtained, for Fe III $3d^6$, a mean error of 988 cm^{-1}!

TABLE III. Interaction-parameter values, in cm^{-1} (GLS1 and GLS2).

Parameter	GLS1	GLS2
A_2	8759 ±28	8762 ±21
A_3	17382 ±26	17385 ±20
A_4	25741 ±22	25736 ±17
A_5	43611 ±14	43597 ±11
A_6	27876 ±20	27861 ±16
A_7	21261 ±14	21259 ±11
A_8	12444 ±23	12433 ±18
B_0	1264.39 ±0.42	1264.38 ±0.32
B_1	51.72 ±0.33	51.66 ±0.25
C_0	4820.1 ±4.1	4821.8 ±3.1
C_1	262.2 ±2.7	262.8 ±2.1
α_0	44.18 ±0.59	44.12 ±0.45
α_1	3.39 ±0.42	3.51 ±0.32
β_0	−392.3 ±8.2	−393.5 ±6.3
β_1	16.8 ±5.0	16.5 ±3.8
T_0	−6.966±0.061	−6.973±0.046
T_1	0.182±0.042	0.199±0.032
$(T_x)_0$	−1.277±0.089	−1.264±0.068
$(T_x)_1$	−0.391±0.063	−0.370±0.047
ζ_0	707.8 ±3.6	703.5 ±5.0
ζ_1	148.7 ±1.9	139.2 ±2.0
ζ_2	11.3 ±1.2	10.0 ±1.3
$(M^0_{ss})_0=(M^0_{soo})_0$		2.701±0.336
$(M^0_{ss})_1=(M^0_{soo})_1$		0.379±0.282
$(M^2_{ss})_0=(M^2_{soo})_0$		1.323±0.333
$(M^2_{ss})_1=(M^2_{soo})_1$		0.203±0.200
Q^2_0		48.8 ±11.2
Q^2_1		9.78 ±8.91
Q^4_0		[33.2]
Q^4_1		[6.65]
Δ	35	27

2. *Variation of the parameter values with N (along the row)*

Table XI lists the values of the various electrostatic parameters, real and effective, obtained in three different SI calculations: (a) LS1 calculations, (b) GLS1, (c) calculations including α, β, and T but omitting T_x.[35–40] Inspection of this table leads to the following conclusions.

(1) In calculations (c) performed without T_x, the parameters change along the row in an irregular fashion, as can be seen by a close inspection of Table XI. This irregular behavior is so pronounced for β, that its mode of change with N remains completely undefined. To some extent this phenomenon also occurs for T. The deviations from regularity reach their peak in Cu V $3d^7$ (see again Table XI). In trying to overcome this problem, Hansen

TABLE IV. Observed and calculated energy levels of Cr V $3d^2$ in cm^{-1} (GLS2).

Obs.	Calc.	$O-C$	J	Term composition	$O-C$ (GLS1)
0.0	−12	12	2	^3F (100%)	−5
508.2	499	9	3	(100%)	8
1141.7	1139	3	4	(100%)	10
13188.0	13182	6	2	^1D (100%)	−1
15491.8	15505	−13	0	^3P (100%)	−5
15676.6	15687	−10	1	(100%)	4
16041.0	16060	−19	2	(100%)	−26
22019.2	22015	4	4	^1G (100%)	2
51146.4	51138	8	0	^1S (100%)	14

TABLE V. Observed and calculated energy levels of Mn V $3d^3$ in cm^{-1} (GLS2).

Obs.	Calc.	$O-C$	J	Term composition	$O-C$ (GLS1)
0.0	11	−11	$\frac{3}{2}$	^4F (100%)	1
359.0	367	−8	$\frac{5}{2}$	(100%)	2
835.1	844	−9	$\frac{7}{2}$	(100%)	−8
1412.2	1422	−10	$\frac{9}{2}$	(100%)	−29
16434.0	16425	9	$\frac{1}{2}$	^4P (100%)	−18
16594.6	16581	14	$\frac{3}{2}$	(98%)	1
17048.6	17034	15	$\frac{5}{2}$	(100%)	28
17892.4	17889	3	$\frac{7}{2}$	^2G (100%)	3
18398.8	18393	6	$\frac{9}{2}$	(98%)	−2
22918.8	22918	1	$\frac{3}{2}$	^2P (62%)+^2_3D (28%)+^2_1D (8%)	−6
23081.6	23076	6	$\frac{1}{2}$	(100%)	5
24630.0	24626	4	$\frac{5}{2}$	^2_3D (80%)+^2_1D (20%)	2
24670.5	24663	7	$\frac{3}{2}$	(49%)+^2P (36%)+^2_1D (14%)	27
24974.8	24962	13	$\frac{9}{2}$	^2H (98%)	28
25333.8	25321	13	$\frac{11}{2}$	(100%)	4
40423.3	40420	3	$\frac{7}{2}$	^2F (100%)	−24
40707.1	40699	8	$\frac{5}{2}$	(100%)	44
62608.2	62637	−29	$\frac{5}{2}$	^2_1D (80%)+^2_3D (20%)	−26
62853.5	62886	−32	$\frac{3}{2}$	(77%)+^2_3D (23%)	−34

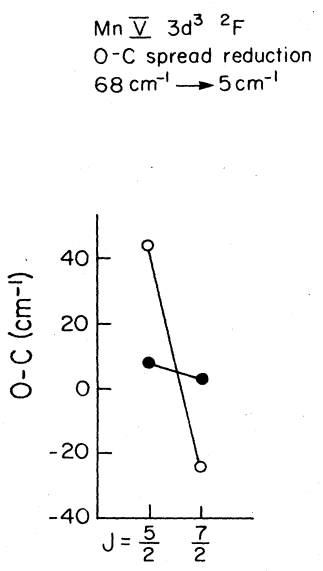

FIG. 1. Improvement of the Mn V $3d^3\,^2F$ splitting due to the additional SDI (○, without the SDI; ●, including the SDI).

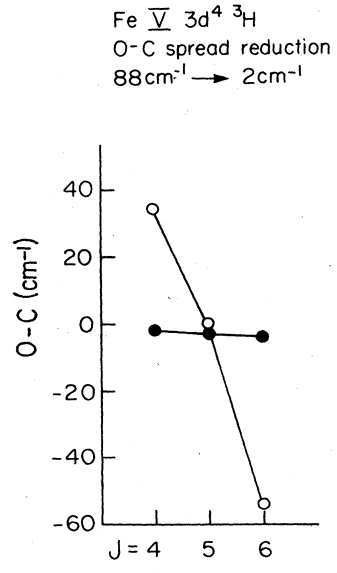

FIG. 2. Improvement of the Fe V $3d^4\,^3H$ splitting due to the additional SDI (○, without the SDI; ●, including the SDI).

TABLE VI. Observed and calculated energy levels of Fe V $3d^4$ in cm^{-1} (GLS2).

Obs.	Calc.	$O-C$	J	Term composition	$O-C$ (GLS1)
0.0	−25	25	0	^5D (100%)	42
142.1	120	22	1	(100%)	38
417.3	397	20	2	(100%)	31
803.1	786	17	3	(100%)	14
1282.8	1267	16	4	(100%)	−14
24055.4	24074	−19	0	^3_4P (60%)+^3_2P (40%)	−30
24972.9	24988	−16	1	(60%)+^3_2P (40%)	−8
26468.3	26483	−15	2	(60%)+^3_2P (40%)	−21
24932.5	24935	−2	4	^3H (97%)	34
25225.9	25229	−3	5	(98%)	0
25528.5	25533	−4	6	(100%)	−54
26760.7	26776	−15	2	^3_4F (78%)+^3_2F (22%)	−2
26842.3	26856	−14	3	(75%)+^3_2F (20%)	−8
26974.0	26985	−11	4	(75%)+^3_2F (19%)	−31
29817.1	29834	−17	3	^3G (95%)	17
30147.0	30166	−19	4	(94%)	−21
30430.1	30450	−20	5	(98%)	−45
36586.3	36550	36	4	^1_4G (65%)+^1_2G (33%)	41
36630.1	36657	−27	3	^3D (100%)	−44
36758.5	36787	−28	2	(99%)	−37
36925.4	36950	−25	1	(100%)	−4
37511.7	37488	24	6	^1I (100%)	23
39633.4	39590	43	0	^1_4S (78%)+^1_0S (21%)	37
46291.2	46270	21	2	^1_4D (78%)+^1_2D (21%)	24
52732.7	52727	6	3	^1F (99%)	0
61854.4	61847	7	2	^3_2P (60%)+^3_4P (39%)	−5
62914.2	62898	16	1	(60%)+^3_4P (30%)	36
63420.0	63403	17	0	(60%)+^3_4P (40%)	29
62238.1	62292	−54	4	^3_2F (80%)+^3_4F (20%)	−45
62321.1	62374	−53	2	(78%)+^3_4F (22%)	−69
62364.4	62415	−51	3	(78%)+^3_4F (21%)	−49
71280.3	71256	24	4	^1_2G (66%)+^1_4G (34%)	23
93832.3	93833	1	2	^1_2D (78%)+^1_4D (22%)	−3
121130.2	121030	100	0	^1_0S (79%)+^1_4S (21%)	101

and Raassen[40] carried out two different least-squares calculations: one with T fixed on some extrapolated value, whereas in the other all parameters were free to change—see Table XI. Since neither of these calculations gave satisfactory results, they concluded that the $3d^7$ configuration "seems to give an example of the breakdown of the linear theory," a theory "which predicts that the parameters vary regularly with N."

(2) The parameter values obtained in LS1 and in GLS1 closely agree with each other. Moreover, the values obtained in GLS1 always (with only one exception) lie within the range of uncertainty of the LS1 parameters. This leads to the conclusion that *the mere introduction of* T_x, in the individual energy-level calculations (LS1), *results in a regular variation with N, of all electrostatic parameters.* The only remaining role of the GLS is to smooth out the N dependence, and also to fix the values of indeterminate parameters in special cases: for example, T and T_x for $N=2,8$, or any parameter depending on (partially) missing experimental data. Returning to β and T, their mode of variation with N is now completely determined: the absolute values of both parameters decrease with N.

(3) Contrary to the behavior of β and T, the absolute values of T_x increase with N, in analogy with α. This property of T_x explains the fact that the irregular behavior of the parameters, in calculations without T_x, is more pronounced on the right-hand side of the row. It also accounts for the greater reductions of the mean errors (Δ_{LS1} as compared with $\Delta_{\alpha\beta T}$) on the right-hand side of the row, on the inclusion of T_x (see Sec. IV A 1 above).

TABLE VII. Observed and calculated energy levels of Co V $3d^5$ in cm^{-1} (GLS2).

Obs.	Calc.	$O-C$	J	Term composition	$O-C$ (GLS1)
0.0	−128	128	$\frac{5}{2}$	^6S (100%)	116
37 217.5	37 209	8	$\frac{11}{2}$	^4G (100%)	−57
37 288.8	37 279	10	$\frac{9}{2}$	(100%)	−1
37 289.5	37 272	17	$\frac{5}{2}$	(100%)	83
37 304.0	37 291	13	$\frac{7}{2}$	(100%)	46
40 753.2	40 792	−39	$\frac{5}{2}$	^4_3P (92%)	−49
40 890.9	40 932	−41	$\frac{3}{2}$	(94%)	−39
41 023.8	41 072	−48	$\frac{1}{2}$	(98%)	−47
44 709.1	44 712	−3	$\frac{7}{2}$	^4D (100%)	−25
44 907.5	44 912	−4	$\frac{1}{2}$	(98%)	30
44 984.1	44 993	−9	$\frac{5}{2}$	(93%)	−20
44 986.7	44 994	−7	$\frac{3}{2}$	(94%)	5
54 339.2	54 316	23	$\frac{11}{2}$	^2I (100%)	68
54 376.6	54 358	19	$\frac{13}{2}$	(100%)	−25
57 082.6	57 059	24	$\frac{5}{2}$	^2_5D (55%)+^2_3F (27%)+^2_1D (18%)	35
57 823.2	57 803	20	$\frac{3}{2}$	(72%)+^2_1D (22%)	12
59 454.9	59 444	11	$\frac{7}{2}$	^2_3F (95%)	−14
60 532.2	60 537	−5	$\frac{5}{2}$	(55%)+^4F (29%)+^2_5D (11%)	8
60 830.3	60 890	−60	$\frac{9}{2}$	^4_3F (97%)	−80
60 973.6	61 029	−55	$\frac{7}{2}$	(96%)	−50
61 213.2	61 264	−51	$\frac{3}{2}$	(94%)	−41
61 284.5	61 315	−30	$\frac{5}{2}$	(69%)+^2_3F (17%)+^2_5D (10%)	−12
64 742.3	64 741	1	$\frac{9}{2}$	^2_3H (78%)+^2_5G (20%)	23
65 283.8	65 284	0	$\frac{11}{2}$	(98%)	−25
66 228.7	66 222	7	$\frac{7}{2}$	^2_5G (98%)	−1
66 760.4	66 755	5	$\frac{9}{2}$	(76%)+^2_3H (21%)	13
70 502.5	70 495	7	$\frac{5}{2}$	^2_5F (99%)	29
70 652.8	70 648	5	$\frac{7}{2}$	(97%)	−14
76 864.5	76 871	−6	$\frac{1}{2}$	^2S (100%)	−9
85 573.5	85 593	−19	$\frac{3}{2}$	^2_3D (100%)	24
85 636.2	85 650	−14	$\frac{5}{2}$	(100%)	−43
95 708.7	95 738	−29	$\frac{9}{2}$	^2_3G (100)%	−16
95 726.5	95 752	−25	$\frac{7}{2}$	(100%)	−42
115 437.1	115 408	29	$\frac{3}{2}$	^2_3P (100%)	49
115 468.5	115 435	33	$\frac{1}{2}$	(100%)	−5
125 022.7	124 986	37	$\frac{5}{2}$	^2_1D (76%)+^2_5D (23%)	68
125 068.8	125 022	47	$\frac{3}{2}$	(76%)+^2_5D (23%)	7

TABLE VIII. Observed and calculated energy levels of Ni V $3d^6$ in cm^{-1} (GLS2).

Obs.	Calc.	$O-C$	J	Term composition	$O-C$ (GLS1)
0.0	−27	27	4	^5D (100%)	−13
889.7	869	21	3	(100%)	15
1489.9	1471	19	2	(100%)	28
1871.5	1854	17	1	(100%)	36
2057.6	2040	18	0	(100%)	40
26 153.0	26 157	−4	2	^3_4P (62%)+^3_2P (37%)	−12
28 697.6	28 708	−10	1	(62%)+^3_2P (36%)	−4
29 640.0	29 657	−17	0	(62%)+^3_2P (36%)	−24
27 111.2	27 114	−3	6	^3H (100%)	−61
27 578.2	27 577	1	5	(97%)	14
27 858.8	27 851	8	4	(89%)	70
29 123.7	29 128	−4	4	^3_4F (68%)+^3_2F (20%)	−14
29 570.8	29 574	−3	3	(76%)+^3_2F (20%)	8
29 899.2	29 902	−3	2	(80%)+^3_2F (20%)	14
33 256.5	33 277	−20	5	^3G (97%)	−61
34 061.7	34 085	−23	4	(93%)	−35
34 416.4	34 435	−19	3	(96%)	15
41 252.2	41 217	35	6	^1I (100%)	32
41 626.9	41 638	−11	2	^3D (97%)	−22
41 701.1	41 710	−9	1	(100%)	18
41 920.2	41 933	−13	3	(100%)	−27
42 208.1	42 180	28	4	^1_4G (65%)+^1_2G (32%)	18
47 699.7	47 658	42	0	^1_4S (76%)+^1_0S (22%)	42
48 607.0	48 583	24	2	^1_4D (76%)+^1_2D (21%)	27
57 924.1	57 905	19	3	^1F (98%)	22
66 737.8	66 758	−20	0	^3_2P (63%)+^3_4P (36%)	−22
67 547.9	67 566	−18	1	(63%)+^3_4P (36%)	3
69.156.1	69 177	−21	2	(62%)+^3_4P (38%)	−37
68 632.1	68 654	−22	2	^3_2F (80%)+^3_4F (20%)	−52
68 718.7	68 751	−32	4	(78%)+^3_4F (21%)	−23
68 854.7	68 879	−24	3	(78%)+^3_4F (20%)	−30
77 899.5	77 909	−9	4	^1_2G (65%)+^1_4G (33%)	−1
104 420.5	104 392	28	2	^1_2D (78%)+^1_4D (22%)	27
	134 313		0	^1_0S (77%)+^1_4S (22%)	

3. *Conclusion A*

The above discussion clearly shows that consistent and reliable values for all electrostatic parameters can only be obtained through the introduction of the complete effective electrostatic interaction represented by α, β, T, and T_x.

B. Stage 2: The additional SDI

1. *Improvement of the calculated multiplet splittings*

On inspecting the O_i-C_i deviations obtained in GLS1 and listed in the last column of Tables IV–X, one can see their pronounced magnetic character, thus calling for the inclusion, in the energy-level calculations, of the additional SDI. The GLS2 calculations, which included the additional SDI, were carried out with 160 levels against 28 parameters (see the third column of Table III). Indeed, the introduction of the additional SDI greatly improved the fit between observed and calculated multiplet splittings, as can be seen on comparing the third and the last columns of Tables IV–X. As demonstrated in these tables, the effects of the SDI is to practically equalize the deviations between calculated and observed levels, for all levels belonging to the same multiplet. Thus, the deviations of magnetic character are almost entirely eliminated, and the remaining deviations are mainly of a purely electrostatic character. These remaining deviations prevent the mean errors obtained in the LS2 and GLS2 calculations from fully reflecting the improvement in the fit due to the additional SDI. In GLS2 the mean error Δ_{GLS2} is 27 cm^{-1} as compared with $\Delta_{GLS1}=35$ cm^{-1}; the mean errors Δ_{LS2} obtained in the separate LS2 calculations are compared with

TABLE IX. Observed and calculated energy levels of Cu V $3d^7$ in cm^{-1} (GLS2).

Obs.	Calc.	$O-C$	J	Term composition	$O-C$ (GLS1)
0.0	13	−13	$\frac{9}{2}$	^4F (100%)	−45
1615.9	1631	−15	$\frac{7}{2}$	(100%)	−14
2759.3	2776	−17	$\frac{5}{2}$	(100%)	0
3528.1	3546	−18	$\frac{3}{2}$	(100%)	8
20826.8	20816	11	$\frac{5}{2}$	^4P (100%)	32
21065.9	21050	16	$\frac{3}{2}$	(90%)	13
21935.1	21923	12	$\frac{1}{2}$	(96%)	−33
22575.3	22572	3	$\frac{9}{2}$	^2G (97%)	14
24099.8	24097	3	$\frac{7}{2}$	(100%)	6
27015.9	27008	8	$\frac{3}{2}$	^2P (78%)+^4P (10%)+^2_3D (9%)	15
28366.6	28359	8	$\frac{1}{2}$	(96%)	−3
30401.7	30392	10	$\frac{11}{2}$	^2H (100%)	1
31823.4	31807	16	$\frac{9}{2}$	(97%)	20
30966.0	30966	0	$\frac{5}{2}$	^2_3D (76%)+^2_1D (23%)	−1
33292.4	33294	−2	$\frac{3}{2}$	(70%)+^2_1D (18%)+^2P (11%)	−11
49490.0	49496	−6	$\frac{5}{2}$	^2F (100%)	54
50071.9	50086	−14	$\frac{7}{2}$	(100%)	−59
76838.2	76837	1	$\frac{3}{2}$	^2_1D (80%)+^2_3D (20%)	−14
77668.0	77671	−3	$\frac{5}{2}$	(76%)+^2_3D (23%)	17

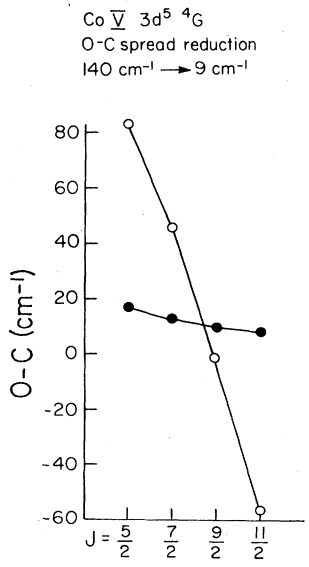

FIG. 3. Improvement of the Co V $3d^5{}^4G$ splitting due to the additional SDI (○, without the SDI; ●, including the SDI).

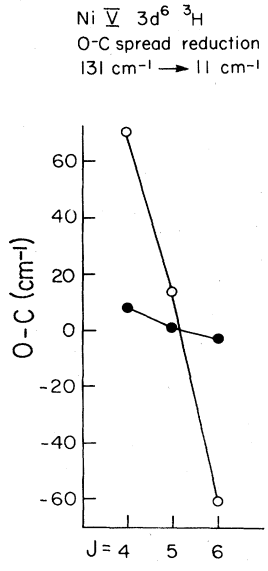

FIG. 4. Improvement of the Ni V $3d^6{}^3H$ splitting due to the additional SDI (○, without the SDI; ●, including the SDI).

TABLE X. Observed and calculated energy levels of Zn V $3d^8$ in cm^{-1} (GLS2).

Obs.	Calc.	$O-C$	J	Term composition	$O-C$ (GLS1)
0.0	11	−11	4	^3F (100%)	−6
2466.0	2468	−2	3	(100%)	−8
4036.0	4035	1	2	(98%)	−16
18 400.0	18 409	−9	2	^1D (78%)+^3P (20%)	−5
22 663.0	22 670	−7	2	^3P (80%)+^1D (20%)	−73
23 107.0	23 108	−1	1	(100%)	40
23 510.0	23 514	−4	0	(100%)	28
30 600.0	30 590	10	4	^1G (100%)	7
69 904.0	69 880	24	0	^1S (100%)	33

Δ_{LS1} at the bottom of Table II.

In order to measure the improvement in the calculated multiplet splittings due to the inclusion of the additional SDI, a different criterion is used. This criterion is referred to as "observed minus calculated ($O-C$) spread."[2–4,28,30] This is defined as the absolute value of the difference between the maximum and the minimum deviations, for levels belonging to the same multiplet. Table XII and Figs. 1–6 demonstrate the reductions in the $O-C$ spreads of several multiplets. The overall improvement in the calculated multiplet structure due to the inclusion of the additional SDI can be seen by comparing the sums of the $O-C$ spreads for all the terms of all the investigated configurations: this sum reduced from 2219 cm^{-1} in GLS1 to 294 cm^{-1} in GLS2, that is, by a factor of 7.5!

TABLE XI. Electrostatic parameters, "real" and effective, as obtained in (a) LS1 calculations, (b) GLS1, (c) calculations including α, β, and T, but neglecting T_x (Refs. 35–40). In cm^{-1}.

Parameter	Cr V $3d^2$	Mn V $3d^3$	Fe V $3d^4$	Co V $3d^5$	Ni V $3d^6$	Cu V $3d^7$[a]	Zn V $3d^8$
F^2_{LS1}	82 658	86 952	91 309	95 709	100 066	104 440	108 843
F^2_{GLS1}	82 587	86 946	91 325	95 696	100 065	104 435	108 805
$F^2_{\alpha\beta T}$	82 493±53	86 067±74	91 393±86	95 815±37	100 231±103	{104 326±101 / 104 177±139}	108 805±180
F^4_{LS1}	50 831±88	54 125±78	57 401±92	60 678±73	64 076±93	67 423±197	70 667±401
F^4_{GLS1}	50 822	54 126	57 430	60 733	64 037	67 341	70 644
$F^4_{\alpha\beta T}$	50 793±88	54 257 ±80	57 705±117	61 111±72	64 733±163	{68 212±154 / 67 824±299}	71 510±401
α_{LS1}	34.5±1.1	37.7±1.2	41.2±1.2	44.6±0.9	47.0±1.0	51.5±2.2	57.0±4.1
α_{GLS1}	34.0	37.4	40.8	44.2	46.6	51.0	54.4
$\alpha_{\alpha\beta T}$	36.1±1.1	37.4±1.5	38.6±1.8	43.0±0.9	45.2±2.2	{50.4±1.9 / 54.9±3.5}	53.0±4.0
β_{LS1}	−419±10	−428±21	−392±18	−396±10	−385±18	−364±26	−327±41
β_{GLS1}	−443	−426	−409	−392	−376	−359	−342
$\beta_{\alpha\beta T}$	−425±10	−476±16	−456±21	−464±10	−513±31	{−414±24 / −359±43}	−450±41
T_{LS1}	[−7.54]	−7.32±0.16	−7.10±0.11	[−6.96]	−6.83±0.09	−6.57±0.22	[−6.31]
T_{GLS1}	−7.51	−7.33	−7.15	−6.97	−6.78	−6.60	−6.42
$T_{\alpha\beta T}$	[−7.3]	−7.2±0.2	−7.3±0.2	[−7.1]	−7.0±0.2	{[−6.8] / −6.3 ±0.4}	[−6.7]
$(T_x)_{LS1}$	[−0.55]	−0.70±0.25	−0.86±0.15	[−1.28]	−1.70±0.16	−1.84±0.38	[−2.00]
$(T_x)_{GLS1}$	−0.1	−0.50	−0.89	−1.28	−1.67	−2.06	−2.45
Δ_{LS1}	14	21	39	44	34	33	47
$\Delta_{\alpha\beta T}$	14	27	58	44	78	{57 / 55}	47

[a]For Cu V $3d^7$ two calculations were carried out (Ref. 40): one with T fixed on −6.8 cm^{-1}, whereas in the other all parameters were free to change in the least-squares calculations. Both sets of results are listed here.

TABLE XII. $O-C$ spread for several selected multiplets (cm^{-1}).

Ion and configuration	Level	Obs.	GLS1 $O-C$	GLS1 $O-C$ spread	GLS2 $O-C$	GLS2 $O-C$ spread
Mn V $3d^3$	$^2F_{7/2}$	40423.3	−24	68	3	5
	$^2F_{5/2}$	40707.1	44		8	
Fe V $3d^4$	$^3H_4$	24932.5	34		−2	
	$^3H_5$	25225.9	0	88	−3	2
	$^3H_6$	25528.5	−54		−4	
Co V $3d^5$	$^4G_{11/2}$	37217.5	−57		8	
	$^4G_{9/2}$	37288.8	−1	140	10	9
	$^4G_{7/2}$	37304.0	46		13	
	$^4G_{5/2}$	37289.5	83		17	
Ni V $3d^6$	$^3H_6$	27111.2	−61		−3	
	$^3H_5$	27578.2	14	131	1	11
	$^3H_4$	27858.8	70		8	
Cu V $3d^7$	$^2F_{5/2}$	49490.0	54	113	−6	8
	$^2F_{7/2}$	50071.9	−59		−14	
Zn V $3d^8$	$^3P_2$	22663.0	−73		−7	
	$^3P_1$	23107.0	40	113	−1	6
	$^3P_0$	23510.0	28		−4	

2. *Modes of change of the various interaction parameters*

The results of stage-2 calculations (see Tables I–III) lead to the following conclusions concerning the modes of change of the various interaction parameters with N (along the row).

(1) The electrostatic as well as the spin-dependent parameters vary regularly with N.

TABLE XIII. Variations of the various interaction parameters along the row, given by the expression $[P(\text{Cu V } 3d^7)/P(\text{Mn V } 3d^3)]^x$. $x=1$, $\frac{1}{4}$, $\frac{1}{3}$, and $\frac{1}{4}$, for the electrostatic, spin-orbit, mutual magnetic, and effective EL-SO parameters.

Parameter	$[P(\text{Cu V } 3d^7)/P(\text{Mn V } 3d^3)]^x$ LS	GLS	HF	PP
B	1.18	1.18	1.20	1.19
C	1.25	1.24	1.19	1.17
F^2	1.20	1.20	1.20	1.18
F^4	1.25	1.24	1.19	1.17
ζ	1.23	1.23	1.24	1.22
M^0	1.21	1.21	1.22	1.21
M^2	1.18	1.24	1.22	1.21
Q^2	1.21	1.24		1.17

(2) There is a close agreement between the parameter values obtained in the LS2, the GLS2, and the *ab initio* calculations.

(3) The variation with N of the real electrostatic parameters F^k (or B,C) and of the magnetic parameters ζ and the M^k's agrees with their theoretical dependence on the effective nuclear charge Z_{eff}. On assuming a Coulomb potential and hydrogenic eigenfunctions, one obtains that[48] (a) the real electrostatic parameters F^k are proportional to Z_{eff}, (b) the spin-orbit parameter ζ_{nl} is proportional to Z_{eff}^4, and (c) the mutual magnetic parameters M^k are proportional to Z_{eff}^3. A comparison of the values of F^2, F^4 (or B,C), ζ, M^0, and M^2 in Cu V $3d^7$ and in Mn V $3d^3$ yields the ratios $[P(\text{Cu V } 3d^7)/P(\text{Mn V } 3d^3)]^x$ (where $x=1$, $\frac{1}{4}$, and $\frac{1}{3}$ for the electrostatic, spin-orbit, and mutual magnetic parameters, respectively), and is given in Table XIII. The equality of these ratios confirms the predicted theoretical behavior of the above mentioned parameters.

(4) The Q^k's comprise sums of products of $R^k(3d\,3d,3dnd)$, $\zeta_{3d,nd}$, and $1/E_{3d,nd}$. Table XIV shows the variations with N of $R^2(3d\,3d,3dnd)$, $(\zeta_{3d,nd})^{1/4}$, and $\Delta E_{3d,nd}$ (for $n=4$–9), by listing the ratios $P(\text{Cu V } 3d^7)/P(\text{Mn V } 3d^3)$ for each of these quantities. These ratios are directly obtained by exploiting the information given in in Tables XVII and XXI. A comparison of the ratios listed in Table XIV with those of the Table XIII shows that $R^2(3d\,3d,3dnd)$, and $\zeta_{3d,nd}$ are, respectively, proportional to Z_{eff} and Z_{eff}^4 (within the corresponding $3d^N$ configuration), in analogy with the internal Slater and spin-orbit parameters. $\Delta E_{3d,nd}$ is found to be proportional to Z_{eff}. This leads to the conclusion that Q^2 is pro-

TABLE XIV. Variations of $R^2(3d\,3d,3dnd)$, $(\zeta_{3d,nd})^{1/4}$, $\Delta E_{3d,nd}$, and $(Q^2_{3d,nd})^{1/4}$ along the row, given by the ratio $P(\text{Cu V } 3d^7)/P(\text{Mn V } 3d^3)$. [$P$ stands for R^2, $\zeta^{1/4}$, ΔE, and $(Q^2)^{1/4}$, respectively.]

	Quantity			
n	$R^2(3d\,3d,3dnd)$	$(\zeta_{3d,nd})^{1/4}$	$\Delta E_{3d,nd}$	$(Q^2_{3d,nd})^{1/4}$
4	1.16	1.19	1.25	1.16
5	1.20	1.18	1.22	1.18
6	1.22	1.18	1.21	1.19
7	1.24	1.18	1.20	1.19
8	1.25	1.18	1.19	1.19
9	1.25	1.17	1.19	1.19
Quantity average	1.22	1.18	1.21	1.18

portional to Z^4_{eff}. The same conclusion is also reached for Q^4. The Z^4_{eff} dependence of the Q^k's is also confirmed by the results of the SI calculations listed in Table XIII.

(5) Tables I and II also give the ratios F^2/F^4, M^0/M^2, and Q^4/Q^2 as obtained by using both the semiempirical and the *ab initio* methods. Inspection of these tables shows that the semiempirical values of F^2/F^4 and M^0/M^2 are almost constant along the row, and close to the constant HF ratios. $(Q^2/Q^4)_{\text{PP}}$ are also constant. The constancy of all these ratios is an immediate result of conclusions (3) and (4). (Since, as mentioned above, Q^4/Q^2 was fixed in the LS2 and GLS2 calculations, these supply no further information.)

3. *Strengths of the additional SDI*

The contribution ΔE_i^{int} of each interaction to a particular energy level E_i is given by the following formula:

$$\Delta E_i^{\text{int}} = \sum_{P_{\text{int}}} (P_{\text{int}} v) \frac{\partial E_i}{\partial P_{\text{int}}} ,$$

where P_{int} are the various parameters representing the interaction under discussion, v represents their numerical value and $\partial E_i/\partial P_{\text{int}}$ is the derivative of E_i with respect to P_{int}. The derivatives are computed in the diagonalization program, together with the calculated energy levels. The separate contributions of the various additional SDI to the splittings of several selected multiplets are given in Table XV. The deviations $O_i - C_i$ before and after the introduction of the additional SDI are also given for comparison. It is clearly seen how the various contributions combine to reduce the $O-C$ spread of the multiplets. For each interaction, Table XV also lists its total contribution to the multiplets under discussion. The total contribution,

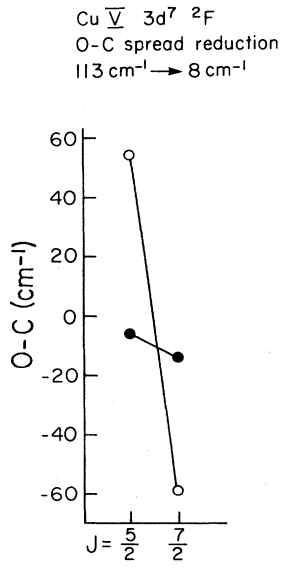

FIG. 5. Improvement of the Cu V $3d^7\,^2F$ splitting due to the additional SDI (○, without the SDI; ●, including the SDI).

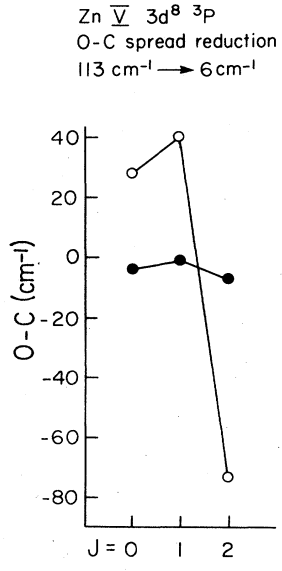

FIG. 6. Improvement of the Zn V $3d^8\,^3P$ splitting due to the additional SDI (○, without the SDI; ●, including the SDI).

TABLE XV. Separate contributions of the various additional SDI to the splittings of several selected multiplets (cm^{-1}).

Configuration	Level	ΔE (ss)	ΔE (soo)	ΔE (ss + soo)	ΔE (EL-SO)	ΔE (total)	$O-C$ (GLS1)	$O-C$ (GLS2)
Mn V $3d^3$	$^2F_{7/2}$	0	−26	−26	2	−24	−24	3
	$^2F_{5/2}$	0	35	35	−2	33	44	8
	$^2F_{5/2}$-$^2F_{7/2}$	0	61	61	−4	57	68	5
Fe V $3d^4$	$^3H_4$	−3	70	67	−16	51	34	−2
	$^3H_5$	3	11	14	−3	11	0	−3
	$^3H_6$	−1	−62	−63	14	−49	−54	−4
	$^3H_4$-$^3H_6$	−2	132	130	−30	100	88	2
Co V $3d^5$	$^4G_{11/2}$	−1	−81	−82	18	−64	−57	8
	$^4G_{9/2}$	1	−7	−6	2	−4	−1	10
	$^4G_{7/2}$	0	54	54	−12	42	46	13
	$^4G_{5/2}$	−5	101	96	−23	73	83	17
	$^4G_{5/2}$-$^4G_{11/2}$	−4	182	178	−41	137	140	9
Ni V $3d^6$	$^3H_6$	−1	−80	−81	21	−60	−61	−3
	$^3H_5$	2	15	17	−3	14	14	1
	$^3H_4$	−6	91	85	−24	61	70	8
	$^3H_4$-$^3H_6$	−5	171	166	−45	121	131	11
Zn V $3d^8$	$^3P_2$	−2	−44	−46	21	−25	−73	−7
	$^3P_1$	14	42	56	14	70	40	−1
	$^3P_0$	−28	85	57	11	68	28	−4
	$^3P_0$-$^3P_2$	−26	129	103	−10	93	101	3
Total contribution[a]		37	675	638	130	508		

[a]The total contribution is defined as the sum of the absolute values of the contributions.

TABLE XVI. Configuration-interaction and effective EL-SO parameter values for Cr V $3d^2$; PP method (cm^{-1}).

Perturbing configuration $3dnd$	$R^2(3d\,3d,3dnd)$	$R^4(3d\,3d,3dnd)$	$\zeta_{3d,nd}$	$\Delta E_{3d,nd}$	Q^2	Q^4
$3d\,4d$	19447	13314	188	319850	16.3	11.2
$3d\,5d$	9493	6487	119	413409	3.9	2.7
$3d\,6d$	6043	4112	85	459857	1.61	1.1
$3d\,7d$	4331	2937	65	486327	0.8	0.5
$3d\,8d$	3321	2246	52	502843	0.5	0.3
$3d\,9d$	2660	1796	43	513840	0.3	0.2
Q^k total					23.4	16.0

TABLE XVII. Configuration-interaction and effective EL-SO parameter values for Mn V $3d^3$; PP method (cm^{-1}).

Perturbing configuration $3d^2nd$	$R^2(3d\,3d,3dnd)$	$R^4(3d\,3d,3dnd)$	$\zeta_{3d,nd}$	$\Delta E_{3d,nd}$	Q^2	Q^4
$3d^2\,4d$	20420	13591	232	341670	19.8	13.2
$3d^2\,5d$	9983	6815	145	437939	4.7	3.2
$3d^2\,6d$	6368	4333	104	485385	1.9	1.3
$3d^2\,7d$	4575	3104	79	512334	1.0	0.7
$3d^2\,8d$	3514	2379	63	529103	0.6	0.4
$3d^2\,9d$	2818	1905	52	540247	0.4	0.3
Q^k total					28.4	19.1

TABLE XVIII. Configuration-interaction and effective EL-SO parameter values for Fe V $3d^4$; PP method (cm^{-1}).

Perturbing configuration $3d^3nd$	$R^2(3d\,3d,3dnd)$	$R^4(3d\,3d,3dnd)$	$\zeta_{3d,nd}$	$\Delta E_{3d,nd}$	Q^2	Q^4
$3d^34d$	21 289	14 512	282	361 146	23.7	16.2
$3d^35d$	10 524	7178	176	460 081	5.8	4.0
$3d^36d$	6758	4598	125	508 478	2.4	1.6
$3d^37d$	4874	3310	96	535 860	1.2	0.8
$3d^38d$	3753	2545	76	552 856	0.7	0.5
$3d^39d$	3015	2042	63	564 130	0.5	0.3
Q^k total					34.3	23.4

TABLE XIX. Configuration-interaction and effective EL-SO parameter values for Co V $3d^5$; PP method (cm^{-1}).

Perturbing configuration $3d^4nd$	$R^2(3d\,3d,3dnd)$	$R^4(3d\,3d,3dnd)$	$\zeta_{3d,nd}$	$\Delta E_{3d,nd}$	Q^2	Q^4
$3d^44d$	22 099	15 036	337	381 571	27.9	19.0
$3d^45d$	11 040	7525	209	483 187	6.8	4.6
$3d^46d$	7132	4854	148	532 526	2.8	1.9
$3d^47d$	5162	3509	113	560 333	1.5	1.0
$3d^48d$	3983	2704	90	577 549	0.9	0.6
$3d^49d$	3204	2174	74	588 950	0.6	0.4
Q^k total					40.5	27.5

TABLE XX. Configuration-interaction and effective EL-SO parameter values for Ni V $3d^6$; PP method (cm^{-1}).

Perturbing configuration $3d^5nd$	$R^2(3d\,3d,3dnd)$	$R^4(3d\,3d,3dnd)$	$\zeta_{3d,nd}$	$\Delta E_{3d,nd}$	Q^2	Q^4
$3d^54d$	22 821	15 505	393	404 876	31.6	21.5
$3d^55d$	11 511	7842	242	509 423	7.8	5.3
$3d^56d$	7476	5089	172	559 759	3.3	2.2
$3d^57d$	5428	3692	131	588 009	1.7	1.2
$3d^58d$	4196	2852	104	605 454	1.0	0.7
$3d^59d$	3379	2296	86	616 984	0.7	0.5
Q^k total					46.1	31.4

TABLE XXI. Configuration-interaction and effective EL-SO parameter values for Cu V $3d^7$; PP method (cm^{-1}).

Perturbing configuration $3d^6nd$	$R^2(3d\,3d,3dnd)$	$R^4(3d\,3d,3dnd)$	$\zeta_{3d,nd}$	$\Delta E_{3d,nd}$	Q^2	Q^4
$3d^64d$	23 600	16 003	461	427 340	36.4	24.7
$3d^65d$	11 959	8136	282	534 467	9.0	6.1
$3d^66d$	7785	5295	200	585 674	3.8	2.6
$3d^67d$	5662	3849	152	614 318	2.0	1.4
$3d^68d$	4381	2976	121	631 967	1.2	0.8
$3d^69d$	3531	2398	99	643 614	0.8	0.5
Q^k total					53.2	36.1

TABLE XXII. Configuration-interaction and effective EL-SO parameter values for Zn V $3d^8$; PP method (cm^{-1}).

Perturbing configuration $3d^7nd$	$R^2(3d\,3d,3dnd)$	$R^4(3d\,3d,3dnd)$	$\zeta_{3d,nd}$	$\Delta E_{3d,nd}$	Q^2	Q^4
$3d^74d$	24 124	16 314	537	446 448	41.5	28.0
$3d^75d$	12 456	8458	329	556 305	10.5	7.1
$3d^76d$	8191	5563	234	608 411	4.5	3.0
$3d^77d$	5983	4063	178	637 424	2.4	1.6
$3d^78d$	4642	3151	142	655 259	1.4	0.9
$3d^79d$	3747	2543	116	667 010	0.9	0.6
Q^k total					61.2	41.2

which can give an indication of the strength of the interaction under discussion, is defined as the sum of the absolute values of the contributions to the individual multiplet splittings. It is thus seen from Table XV that the soo is by far the strongest interaction, as compared with the other additional SDI, and can reach 182 cm^{-1} (for Co V $3d^5\,{}^4G$). The effective EL-SO interaction is weaker than the soo by about a factor of 5 and can reach 45 cm^{-1} (in Ni V $3d^6\,{}^3H$). The ss interaction is the weakest of them all, its strength being more than 1 order of magnitude smaller than that of the soo. Its characteristic contribution is only a few wave numbers per multiplet, its contribution to Zn V $3d^8$ ($^3P_1$-$^3P_0$), which amounts to 42 cm^{-1}, constitutes an exception.

4. Conclusion B

The great importance of the additional SDI as a tool for improving the calculated multiplet splittings has been demonstrated. Consistent values for all appropriate parameters were obtained, and their dependence on the effective nuclear charge was determined. Although the various additional SDI differ in strength, their simultaneous introduction is essential for obtaining the above-mentioned results. On comparing the conclusions obtained in the present work with those obtained in previous works,[3,30] it is interesting to note that the additional SDI have different relative strengths in different spectra: in the third spectra of the iron group the soo and the effective EL-SO interactions are approximately of equal strengths, contributing several tens of cm^{-1} to the multiplet splittings. On moving to the fifth spectra of the iron group (the present work), the soo doubled its strength, whereas the strength of the effective EL-SO did not change. In U V $5f^2$, it was shown that only the effective EL-SO interaction was of importance and the mutual magnetic interactions could be neglected. In all cases, the ss was found to be the weakest interaction of all additional SDI.

[1] Z. B. Goldschmidt, A. Pasternak, and Z. H. Goldschmidt, Phys. Lett. **28A**, 265 (1968).
[2] Z. B. Goldschmidt, J. Phys. (Paris) Colloq. **31**, C4-163 (1970).
[3] A. Pasternak and Z. B. Goldschmidt, Phys. Rev. A **6**, 55 (1972); **9**, 1022 (1974).
[4] Z. B. Goldschmidt, in *Atomic Physics*, edited by J. J. Smith and K. G. Walters (Plenum, New York, 1973), Vol. 3, pp. 221–246.
[5] R. E. Trees, Phys. Rev. **83**, 756 (1951); **84**, 1089 (1951).
[6] G. Racah, Phys. Rev. **85**, 381 (1952).
[7] G. Racah, in proceedings of the Rydberg Centennial Conference [Acta Univ. Lund. **50**, 21 (1955)].
[8] R. F. Bacher and S. Goudsmit, Phys. Rev. **46**, 948 (1934).
[9] G. Racah and Y. Shadmi, Bull. Res. Counc. Isr. Sec. F **8**, 15 (1959).
[10] G. Racah and Y. Shadmi, Phys. Rev. **119**, 156 (1960).
[11] R. E. Trees and C. K. Jorgensen, Phys. Rev. **123**, 1278 (1961).
[12] K. Rajnak and B. G. Wybourne, Phys. Rev. **132**, 280 (1963).
[13] G. Racah and J. Stein, Phys. Rev. **156**, 58 (1967).
[14] R. E. Trees, Phys. Rev. **129**, 1220 (1963).
[15] G. Racah, J. Quant. Spectrosc. Radiat. Transfer **4**, 617 (1964).
[16] B. R. Judd, Physica **33**, 174 (1967).
[17] S. Feneuille, C. R. Acad. Sci. **262**, 23 (1966).
[18] Y. Shadmi, J. Oreg, and J. Stein, J. Opt. Soc. Am. **58**, 909 (1968).
[19] Y. Shadmi, E. Caspi, and J. Oreg, J. Res. Natl. Bur. Stand. (U.S.) **73A**, 173 (1969).
[20] H. A. Bethe and E. E. Salpeter, *Quantum Mechanics of One- and Two-Electron Atoms* (Springer, Berlin, 1957).
[21] C. Slater, *Quantum Theory of Atomic Structure* (McGraw-Hill, New York, 1960), Vol. II.
[22] H. H. Marvin, Phys. Rev. **71**, 102 (1947).
[23] H. Horie, Prog. Theor. Phys. (Kyoto) **10**, 296 (1953).
[24] A. Jucys, R. Dagys, J. Vizbaraite, and S. Zvironaite, Trudy Akad. Nauk. Litovsk SSR B **3**, 53 (1961).
[25] A. P. Jucys and A. J. Savukynas, *Mathematical Foundations*

of the Atomic Theory (Vilnius, 1973), in Russian.
[26]M. Blume and R. E. Watson, Proc. R. Soc. London Ser. A **271**, 565 (1963).
[27]B. R. Judd, H. M. Crosswhite, and Hannah Crosswhite, Phys. Rev. **169**, 130 (1968).
[28]Z. B. Goldschmidt, in *Handbook on the Physics and Chemistry of Rare Earths,* edited by K. A. Gschneider and L. Eyring (North-Holland, Amsterdam, 1978), pp. 1—171.
[29]Hannah Crosswhite, H. M. Crosswhite, and B. R. Judd, Phys. Rev. **174**, A8 (1968).
[30]Z. B. Goldschmidt, Phys. Rev. A **27**, 740 (1983).
[31]C. H. H. Van Deurzen, K. Rajnak, and J. G. Conway, J. Opt. Soc. Am. B **1**, 45 (1984).
[32]B. R. Judd, Comments At. Mol. Phys. **1**, 173 (1970).
[33]J. O. Ekberg, Phys. Scr. **7**, 59 (1973). See also J. Sugar and C. Corliss, J. Phys. Chem. Ref. Data **6**, 317 (1977).
[34]V. I. Kovalev, A. A. Ramonas, and A. N. Ryabtsev, Opt. Spektrosk. **43**, 10 (1977) [Opt. Spectrosc. (USSR) **43**, 4 (1977)]. See also C. Corliss and J. Sugar, J. Phys. Chem. Ref. Data **6**, 1253 (1977).
[35]B. C. Fawcett and H. F. Henrichs, Astron. and Astrophys. Suppl. **18**, 157 (1974); J. O. Ekberg, Phys. Scr. **12**, 42 (1974). See also J. Reader and J. Sugar, J. Phys. Chem. Ref. Data **4**, 353 (1975).
[36]A. J. J. Raassen and Th. A. M. van Kleef, Physica **96C**, 367 (1979). See also J. Sugar and C. Corliss, J. Phys. Chem. Ref. Data **10**, 1097 (1981).
[37]A. J. J. Raassen, Th. A. M. van Kleef, and B. C. Metsch, Physica **84C**, 133 (1976). See also C. Corliss and J. Sugar, J. Phys. Chem. Ref. Data **10**, 197 (1981).
[38]Th. A. M. van Kleef, A. J. J. Raassen, and Y. N. Joshi, Physica **84C**, 401 (1976).
[39]Th. A. M. van Kleef, L. I. Podobedova, A. N. Ryabtsev, and Y. N. Joshi, Phys. Rev. A **25**, 2017 (1982).
[40]J. E. Hansen and A. J. J. Raassen, Physica **111C**, 76 (1981).
[41]B. R. Judd, Jorgen E. Hansen, and A. J. J. Raassen, J. Phys. B **15**, 1457 (1982).
[42]B. R. Judd, *Second Quantization and Atomic Spectroscopy* (Johns Hopkins University, Baltimore, 1967).
[43]G. Racah, Phys. Rev. **62**, 438 (1942).
[44]G. Racah, Phys. Rev. **63**, 367 (1943).
[45]B. R. Judd, *Operator Techniques in Atomic Spectroscopy* (McGraw-Hill, New York, 1963).
[46]C. Froese Fischer, *The Hartree-Fock Method for Atoms* (Wiley, New York, 1977); Comput. Phys. Commun. **14**, 145 (1978).
[47]M. Klapisch, Comput. Phys. Common. **2**, 239 (1971).
[48]E. U. Condon and G. H. Shortley, *The Theory of Atomic Spectra* (Cambridge University, Cambridge, 1953).